Towed Array Shape Estimation Using Kalman Filters—Theoretical Models

Douglas A. Gray, *Member, IEEE,* Brian D. O. Anderson, *Fellow, IEEE,* and Robert R. Bitmead, *Fellow, IEEE*
(Invited Paper)

Abstract— **The dynamical behavior of a thin flexible array towed through the water is described by the Paidoussis equation. By discretizing this equation in space and time a finite dimensional state space representation is obtained where the states are the transverse displacements of the array from linearity in either the horizontal or vertical plane. The form of the transition matrix in the state space representation describes the propagation of transverse displacements down the array. The outputs of depth sensors and compasses located along the array are shown to be related in a simple, linear manner to the states. From this state space representation a Kalman filter is derived which recursively estimates the transverse displacements and hence the array shape. It is shown how the properties of the Kalman filter reflect the physics of the propagation of motion down the array. Solutions of the Riccati equation are used to predict the mean square error of the Kalman filter estimates of the transverse displacements.**

Index Terms—**Towed arrays, array shape estimation, Paidoussis equation, Kalman filter.**

I. Introduction

THIN flexible arrays of hydrophones are becoming increasingly important in sonar and seismic applications [1], [2]. In both fields, the trend in array development is to make arrays longer and thinner. This trend tends to exacerbate a major problem with towed arrays; that of accurately knowing the shape of the array at any given instant of time. Ideally, the array is designed to be linear, however, transverse motion of the towing vessel, oceanic currents, and hydrodynamic effects all contribute to transverse displacements of the array from a straight line. Furthermore, nonneutral buoyancy of the array or, worse still, nonuniform changes in the density of the array, can also be a cause of transverse motion of the array.

In many applications, the distortion of the shape of the array has, in the past, been ignored and the array treated as a straight line. However, as the uses and processing of the hydrophone data become more sophisticated the sensitivity to errors in the hydrophone positions, caused by the transverse array motion, becomes more critical. Typical of the more sophisticated towed array processing techniques are adaptive beamforming [3], adaptive cancellation of tow vessel noise [4], bearing estimation using eigenvectors [5], and ranging techniques such as triangulation [6] or wave-front curvature [7].

One way to overcome this problem is to instrument the array with depth sensors and compasses; these give localized vertical and horizontal information of the transverse displacements of the array respectively. As an example, one approach would be to use the outputs of a depth sensor and compass located at each receiver to estimate its position. In practice, however, such a solution is neither mechanically nor economically feasible and often, the number of sensors is too small to be able to directly infer the array shape. One way around this problem is to assume the array shape can be modeled by a low order polynomial and to use the available sensors' information to determine the coefficients of this polynomial; this approach is discussed in detail in [8].

There is evidence, however, that the shape of a towed array at a given instant of time can be partially inferred by its shape at earlier times [9], [29]. This property can then be used to estimate the transverse displacement of the array at points where depth sensors or compasses are not located. For example, there is considerable evidence that motion induced at the tow point, termed TPI motion, propagates down the array and, for disturbances whose typical wavelengths are long compared with the length of the array, the propagation speed is the tow speed of the array and furthermore that these disturbances are lightly damped [9]. If this where the case, in the absence of errors, one sensor at the head of the array would provide estimates of the shape of the array. In general, the propagation of motion down the array, for an idealized two-dimensional problem, is governed by a partial differential equation, known as the Paidoussis equation [10], [11]. This equation, is discussed in Section II, and forms the basis for the method of array shape estimation presented in this paper.

The Paidoussis equation describes the propagation of motion down the array and, by discretizing in time, allows the transverse displacements of a small segment of the array at one instant in time to be related to the displacement of upstream segments at an earlier instant in time. This immediately suggests a discrete-time state space formulation [12], in which the state of the system is a finite dimensional vector whose components are the transverse displacements of each of the

Manuscript received January 20, 1993; revised April 25, 1993. This work was performed while one of the authors (D. A. Gray) visited the Department of Systems Engineering at the Australian National University. This work was supported by the Australian Department of Defence.

D. A. Gray is with the Department of Electrical Engineering, University of Adelaide, Adelaide, South Australia. He is also with the Cooperative Research Centre for Sensor Signal and Information Processing.

B. D. O. Anderson and R. R. Bitmead are with the Department of Systems Engineering, Australian National University, Canberra, ACT, Australia. They are also with the Cooperative Research Centre for Robust and Adaptive Systems.

IEEE Log Number 9211450.

segments. The state transition matrix, describing how the states of the system, i.e., the transverse displacements, at time t are related to the states at time $t-1$, is determined by a discretization of the Paidoussis equation. In this model, TPI motion may be introduced as a driving term in the state space equations, with the boundary conditions of the discretization scheme determining which properties of the driving term are required to be known, e.g., its slope etc. If the driving terms are, as is often the case, not known, then the unknown boundary condition can be treated as an error signal in the model. Also, it can readily be shown that the outputs of either depth sensors or compasses mounted along the array can be linearly related to the state of the system plus the addition of measurement noise. This representation of a system is classical in linear systems analysis and, given such a model, a powerful method for estimating the state of the system from the available measurements is by the use of a Kalman filter [12]. The Kalman filter, at each instant in time, gives the least mean square estimate of the state of the system, when all the previous sampled time history of the measurement sensors (i.e., the compasses and/or depth sensors) is taken into account. Furthermore the Kalman filter can be used to give a prediction of the state, i.e., the array shape, at some later time, a filtered estimate of the state at the present time, or a smoothed estimate of the state at some earlier time.

A particularly attractive feature of the Kalman filter is its robustness to deviations of the actual system from the one used to design the Kalman filter, e.g., model errors, incorrect assumptions about the noise statistics, etc. This property is particularly important in the underwater environment where changes in the prevailing oceanic conditions will certainly introduce errors in the modelling of the array dynamics.

In Section III the array shape estimation problem is formulated within the state space representation. Displacements in only one transverse dimension are considered and the array shape is discretized into a number of equal sized segments. The Paidoussis equation is discretized in both space and time, using first-order differences to obtain a simple and useful finite dimensional state space representation of the system and a Kalman filter for estimating the array shape is derived. From any beamforming applications this approach is sufficient, however, in some applications, where the array is instrumented by compasses and it is bearing information that is desired, a more appropriate form of the state vector is not in terms of transverse displacements, but in terms of the variations of the slope of the array. This problem is discussed in Section IV and it is shown how, if the state vector is taken as the discretized slopes of the array, a state space representation, describing the propagation of the slope down the array, can be obtained which is similar to the displacement representation discussed above.

For disturbances whose wavelengths are comparable or greater than the length of the array, the Paidoussis equation can be shown [13] to reduce to a particularly simple form. The simplified equation predicts that transverse displacements propagate down the array at the tow speed with no damping and this behavior is termed water pully motion. In this case, the form of the state transition matrix is particularly simple and, in Section V, some simple state transition matrices appropriate to water pulley behavior are derived and discussed by way of example. Furthermore, for this model, a particularly simple form of the state transition matrix allows the Riccati equation underpinning the Kalman filter to be solved analytically and provides valuable insight into the functioning of the Kalman filter.

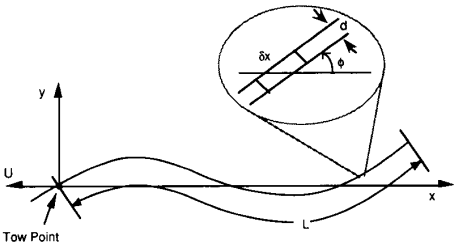

Fig. 1. Two-dimensional tow (vertical scale exaggerated).

II. Description on an Array Towed at a Constant Speed

In this section, the Paidoussis equation, describing the dynamics of a neutrally buoyant array towed at a constant speed through the water is discussed. The array considered is assumed to have a circular cross-section and so, following the arguments of [14], we assume that motion in the horizontal and vertical directions can be treated independently. Thus, attention is restricted to the two-dimensional sub-surface problem; this is illustrated in Fig. 1 with U denoting the horizontal tow speed of the array. Early studies of the dynamics of the uniform flow of a fluid over a flexible cylinder were carried out by Paidoussis [10], [11] who used particular expressions of the drag coefficients, first proposed by Taylor [15], which, when linearized for small attack angles, gave rise to a partial differential equation describing the motion of the cylinder. Paidoussis's approach was to consider a small element, δx, of the array inclined at an angle ϕ to the flow. The assumption is made that the hydrodynamic force acting on δx depends only on the angle that it makes with the flow and is not effected by the curvature of the array near δx nor by flow over the cable. The Paidoussis equation is obtained by (separately) equating to zero the longitudinal and normal components of the forces using linearized expressions for the longitudinal and normal viscous forces [10], [11]. Further understanding of this equation, and its application to the type of arrays that are common in sonar and seismic applications, was furnished by Pao and Tran [16], [17] who considered the stability of the array and Ortloff and Ives, [18], who derived explicit solutions in terms of Bessel functions.

The most extensive analysis of the Paidoussis equation, when applied to towed arrays, has been through the work of Kennedy [9], [13], [19], [20] and more recently by Dowling [21], [22]. In addition to proving the stability of the array in regimes of interest, Kennedy found, by considering various perturbational solutions of the partial differential equations, that for TPI motion with long wavelengths, the description of the array behavior could be considerably simplified. Fur-

thermore, these simplified descriptions appear to describe the experimentally observed behavior of the array [19], [29].

It is worth commenting on the choice of expressions for the drag forces. Paidoussis used expressions which were originally derived by Taylor [15], in a very heuristic fashion, and, as observed by Ortloff and Ives, are only applicable for rough cylinders. Bearing in mind that most sonar and seismic arrays are smooth it is somewhat surprising that they have been used as the basis for all further work. However, when the drag forces for smooth cylinders, again derived by Taylor [15], are used, the linearization procedure implies that the tension is constant over the array [23], which is not particularly realistic. Thus, to obtain a physically sensible linearization, it seems necessary to use expressions for rough arrays. In this case, the greater drag force results in a higher tension at any point along the array than occurs for a smooth array. Since this tension supplies part of the restoring force, it would be expected that the predicted displacements for rough arrays would be less than those for smooth arrays. Indeed, some experimental evidence, presented in [24], supports this conclusion.

The Paidoussis equation, minus a fourth-order bending stiffness term, which, for flexible towed arrays, can be ignored [13], takes the form

$$m\frac{\partial^2 y}{\partial t^2} + M\left[\frac{\partial}{\partial t} + U\frac{\partial}{\partial x}\right]^2 y - \frac{\partial}{\partial x}\left[\left[\frac{1}{2}c_t\left[\frac{L-x}{d}\right] + \frac{1}{2}c_t'\right] \cdot MU^2\frac{\partial y}{\partial x}\right] + \frac{1}{2\pi}c_n\frac{MU}{d}\left[\frac{\partial y}{\partial t} + U\frac{\partial y}{\partial x}\right] = 0$$

where, as illustrated in Fig. 1,

$y = y(t, x)$	the transverse displacement
M	the mass per unit length of the neutrally buoyant cylinder
m	the virtual mass per unit length of the fluid
d	the diameter of the array
U	the tow speed along the x-axis
L	the array length
c_t	the tangential drag coefficient of the cylinder
c_n	the normal drag coefficient of the cylinder

and

c_t' is the coefficient of form drag of the trailing end[1].

The extension to the non-neutrally buoyant array is achieved by incorporating a buoyancy term in the above equations [22]. In common with other workers, the following dimensionless variables are introduced

$$\tau = t\frac{U}{L},\ \beta = \frac{M}{M+m},\ \xi = \frac{x}{L},\ \epsilon = \frac{L}{d}$$

$$\text{and}\quad \eta = \eta(\tau, \xi) = \frac{y(t, x)}{L}.$$

[1]The modeling of the boundary conditions at the trailing end has been treated heuristically by Kennedy [13] who approximated the free trailing end by a tapered section and introduced the term c_t' to model the coefficient of the form drag at the trailing end. (Note that arrays with drogues at the trailing end can be described by substituting an appropriate expression for c_t'.) See also [10], [17], and [18] for a discussion of the trailing end boundary conditions.

The Paidoussis equation then becomes

$$\frac{\partial^2\eta}{\partial\tau^2} + 2\beta\frac{\partial^2\eta}{\partial\xi\partial\tau} + (a + b\xi)\frac{\partial^2\eta}{\partial\xi^2} + c\frac{\partial\eta}{\partial\xi} + e\frac{\partial\eta}{\partial\tau} = 0 \quad (1)$$

where

$$a = \beta(1 - 2c_t\epsilon - 2c_t')$$
$$b = 2\beta c_t\epsilon$$
$$c = 2(c_t + c_n/\pi)\epsilon\beta$$

and

$$e = \frac{2}{\pi}\beta c_n\epsilon.$$

The initial and end boundary conditions were defined by Kennedy as

1) $\eta = 0$ if $\xi = 0$ (i.e., a fixed end and the absence of a driving term)
2) $|\eta|$ is finite if $\xi = 1$ (bounded free end deflection)
3) $\eta = \eta(\xi)$ if $\tau = 0$ (prescribed initial deflection)

and

1) $\eta_{\tau|_{\tau=0}} = 0$ (zero initial transverse speed relative to the origin which is assumed to be moving through the fluid at a constant speed of U).

For all sonar and seismic arrays, $L \gg d$ and thus $\epsilon^{-1} \ll 1$. Following Kennedy, we consider a perturbational expansion in powers of ϵ^{-1}. Thus substituting

$$\eta(\tau, \xi) = \eta_0(\tau, \xi) + \epsilon^{-1}\frac{\partial\eta(\tau, \xi)}{\partial\epsilon^{-1}}\bigg|_{\epsilon^{-1}=0} +, \cdots,$$

in (1), multiplying by ϵ^{-1}, and ignoring terms in ϵ^{-1} we obtain

$$c_t(\xi - 1)\frac{\partial^2\eta_0}{\partial\xi^2} + \left(c_t + \frac{c_n}{\pi}\right)\frac{\partial\eta_0}{\partial\xi} + \frac{c_n}{\pi}\frac{\partial\eta_0}{\partial\tau} = 0. \quad (2)$$

It is this equation, referred to as SDP, i.e., small diameter Paidoussis equation, that we consider in detail in Section IV.

Fig. 2 is an example solution of the Paidoussis equation using expressions derived by Dowling [21]. This example models an array 100 m long towed through the water at a speed of 16 knots and excited at the tow point by a sinusoidal forcing function with a period of 12 s and an amplitude of 5 m. (The array was discretised into 20 segments.) As well be discussed below, for these parameters the transverse displacement propagates down the array at close to the speed of the array through the water and is only lightly damped. Note that in the plotted results the tow point has always been adjusted to be at the origin. This reference frame is the one typically adopted by experimenters, and gives rise to the commonly quoted observation that the array is flexing about its midpoint.

Below, we shall be concerned with a low nondimensional frequency approximation. In nondimensional coordinates, the frequency $\bar{f}$ of the disturbance of frequency f is given by

$$\bar{f} = f\frac{L}{U}.$$

This can be expressed as

$$\bar{f} = fT = \frac{T}{T_f}$$

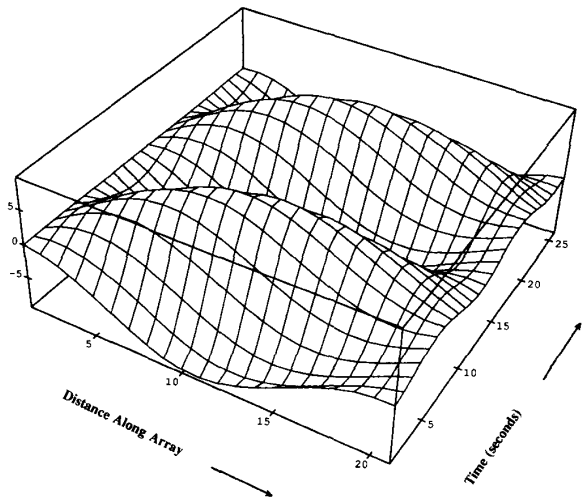

Fig. 2. Example solution of Paidoussis equation.

where T_f is the period of the disturbance, and so $\overline{f}$ is the number of periods of the exciting sinusoid that occur during the time, $T(= L/U)$, in which the array transverses its length. Alternatively, since the speed of the tow point is U and $U = f\lambda$, we have

$$\overline{f} = \frac{L}{\lambda}$$

which is the number of wavelengths of the disturbance that can fit into the array.

To this stage we have assumed that the array is infinitely flexible so that stiffness terms can be ignored and is also thin enough so that the ratio of its diameter to its length is small. By restricting the wavelengths of disturbances propagating down the array to be comparable or greater than the array length, i.e., $\overline{f} < 1$, Kennedy has derived a zeroth-order solution to (1). In this case the solution is governed by an equation of the form

$$\left(c_t + \frac{c_n}{\pi}\right)\frac{\partial \eta}{\partial \xi} + \frac{c_n}{\pi}\frac{\partial \eta}{\partial \tau} = 0 \tag{3}$$

which can be seen to be derived from the SDP equation (2) by assuming the expression

$$\frac{\partial^2 \eta}{\partial \xi^2},$$

i.e., the acceleration of the array in the tow direction, is small. The solution of (3) is easily verified to be

$$\eta(\tau, \xi) = f(\xi - \tilde{\rho}\tau)$$

where $f(x)$ is any function with a continuous first order derivative and $\tilde{\rho}$ is given by

$$\tilde{\rho} = \frac{\pi c_t + c_n}{c_n}. \tag{4}$$

This solution, termed "water pulley" by Kennedy, implies that effects propagate undamped down the array at a speed of $\tilde{\rho}U$. As observed by Kennedy, in many cases $\tilde{\rho}$ is close to unity and so effects do in fact propagate down the array at close to the tow speed of the array. Some recently reported experimental results [29] support the validity of this model.

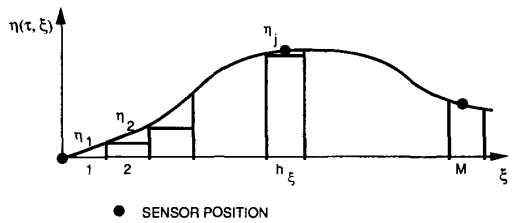

Fig. 3. Spatial discretization of array.

III. Array Shape Estimation Using a Kalman Filter

To design a Kalman filter for estimating the array shape two important equations must be derived. This first is the state equation which describes the time evolution of the states. Thus a finite dimensional, discrete time, state space model [12] for the propagation of tow point induced motion down the array must be derived. This is done by carrying out a spatial and temporal discretization of the following form of the nondimensional small diameter Paidoussis equation

$$(\tilde{\rho} - 1)(\xi - 1)\frac{\partial^2 \eta}{\partial \xi^2} + \tilde{\rho}\frac{\partial \eta}{\partial \xi} + \frac{\partial \eta}{\partial \tau} = 0 \tag{5}$$

where $\tilde{\rho}$ is given by (4). The states of the system are the transverse displacements of a finite straight line segment approximation of the array shape at any instant in time as illustrated in Fig. 3. The second equation is the measurement equation which relates the outputs of either depth sensors or compasses to the system states; this is discussed in Section III.D.

A. Derivation of Transition Matrix

There are many ways of discretizing partial differential equations and here we consider a simple Euler discretization. Even with a simple first order discretization there is a choice of backward versus forward differences etc. In [23] it is shown that for describing tow point induced motion propagating down the array the most natural choice is to use a forward difference for $\frac{\partial}{\partial \tau}$, a backwards difference for $\frac{\partial}{\partial \xi}$, and a backwards difference for $\frac{\partial^2}{\partial \xi^2}$. Note that this is equivalent to a straight line segment approximation to the array shape.

Let h_t and h_ξ denote the temporal and spatial discretization intervals respectively and define $\eta_m(k) = \eta(kh_t, mh_\xi)$ for $m = 1, 2, \cdots, M$ and $k = 1, 2, \cdots$ where $\eta(\tau, \xi)$ is the solution of (5). The following Euler approximations are used

$$\frac{\partial \eta}{\partial \tau} \cong \frac{\eta_m(k+1) - \eta_m(k)}{h_\tau},$$
$$\frac{\partial \eta}{\partial \xi} \cong \frac{\eta_m(k) - \eta_{m-1}(k)}{h_\xi}$$

and

$$\frac{\partial^2 \eta}{\partial \xi^2} = \frac{1}{h_\xi^2}\{\eta_m(k) - 2\eta_{m-1}(k) + \eta_{m-2}(k)\}$$

Replacing the partial differentials in (5) by the above finite difference approximations results in a state equation of the form

$$\underline{\eta}(k+1) = F\underline{\eta}(k) + \underline{u}(k) + \underline{w}(k). \tag{6}$$

As illustrated in Fig. 3, the components of $\underline{\eta}(k)$ are the transverse displacements of each of the M segments of a piecewise linear approximation of the array shape at time kh_τ. The vector $\underline{u}(k)$, see later, can be interpreted as the driving term, or TPI motion, and the vector $\underline{w}(k)$ represents additive noise which can be used to represent various model errors. One example, see later, is when $\underline{w}(k)$ is used to represent errors associated with the discretisation of the partial differential equation.

F is the transition matrix; it relates the displacement of any segment at time kh_τ to the displacement of the two immediate upstream segments of the array at time $(k-1)h_\tau$ and is given by

$$F = (1-\rho)I + \rho L + \rho D(I - 2L + L^2). \tag{7}$$

In the above,

$$\rho = \tilde{\rho}\frac{h_\tau}{h_\xi} \tag{8}$$

D is a diagonal matrix defined by $d = \text{diag}\{\delta_1, \delta_2, \cdots, \delta_M\}$, where

$$\delta_m = \frac{(1 - mh_\xi)(\tilde{\rho} - 1)}{\tilde{\rho}h_\xi},$$

and L is a lower triangular matrix whose only nonzero elements are unity in the first diagonal below the main diagonal, i.e.,

$$L = \begin{bmatrix} 0 & 0 & \cdot & \cdot & 0 \\ 1 & 0 & \cdot & \cdot & \cdot \\ 0 & 1 & 0 & \cdot & \cdot \\ \cdot & \cdot & \cdot & \cdot & \cdot \\ 0 & \cdot & \cdot & 1 & 0 \end{bmatrix}$$

Consideration of the water pulley approximation defines a model with a simpler form of F which can be related to the propagation of effects down the array in a very obvious physical manner. In this case, discretization of (3) results in a transition matrix of the form

$$F = (1-\rho)I + \rho L. \tag{9}$$

The dispersive coefficient, ρ, is governed by $\tilde{\rho}$, h_τ, and h_ξ. As discussed earlier, $\tilde{\rho}$ is the nondimensional speed of propagation of tow point induced motion down the array and, from (9), it can readily be seen that $\rho = 1$ corresponds to the case where the temporal discretization is chosen to be the time that it takes for such a displacement to propagate one spatial discretization interval. In this case, the state space transition matrix becomes L, implying that the transverse displacement of any segment at time kh_τ is simply that of the previous upstream segment at time $(k-1)h_\tau$. In [25] it is suggested that this simplified model may be adequate for many cases of practical interest and that it may be simply augmented by introducing a damping coefficient, α, defined as the damping over a length h_ξ. This extremely simple, but useful, model results in a transition matrix of the form

$$F = \alpha L.$$

B. Driving Terms and Boundary Conditions

In practice, knowledge of the tow point displacement and its shape will depend on the particular situation. For the example of a submarine towing an array and carrying out a specific maneuver, such as a turn, the tow point motion trajectory may be known with some degree of accuracy. Another example is the case of a surface vessel towing a subsurface array with the depth of the head of the subsurface array being controlled by an active leveling device such as the Digicourse 5000 family of "compass birds" [27].

a) Known Driving Term: In the difference equation (6), the displacement of an array segment is related to the displacements of the two immediate upstream segments. For the first two segments this is not possible, and in place of this information, appropriately chosen functions of the tow point induced option are introduced through the driving term, $\underline{u}(k)$, i..e, the approach adopted here is to allow the boundary conditions of the discretization to determine the form of the driving term. From the discretization scheme chosen $\underline{u}(k)$ takes the form

$$\underline{u}^T(k) = [\rho(1+\delta_1)\eta_0(k) + \rho\delta_1(\eta_0(k) - \eta_{-1}(k)), \\ - \rho\delta_2\eta_0(k), 0 \cdots, 0].$$

Thus, to match completely the boundary conditions, not only is the input driving displacement at the tow point of the array, $\eta_0(k)$, required to be known but also the slope, i.e.,

$$\frac{\eta_0(k) - \eta_{-1}(k)}{h_\xi} \equiv \left|\frac{\partial\eta}{\partial\xi}\right|_{\xi=0}$$

is required. Similarly, for the water pulley model, a driving term of the form

$$\underline{u}^T(k) = \rho[\eta_0(k), 0, \cdots, 0]$$

results: in this case it suffices to know the displacement of the tow point.

b) Unknown Driving Term: One approximation for an unknown driving term at the tow point is to model it as a white noise process, ϵ_k, with a known variance σ_u^2. In this case $u(k)$ has the form

$$\underline{u}^T(k) = [\epsilon_k, 0, \cdots, 0]$$

and U, the covariance matrix of the driving term has the form

$$U = \sigma_u^2 \cdot \begin{bmatrix} 1 & 0 & \cdot & \cdot & 0 \\ 0 & 0 & \cdot & \cdot & \cdot \\ \cdot & \cdot & \cdot & \cdot & \cdot \\ \cdot & \cdot & \cdot & \cdot & \cdot \\ 0 & \cdot & \cdot & \cdot & 0 \end{bmatrix}.$$

C. Model Errors

To complete the transition equation an expression for the model error, $\underline{w}(k)$, is needed. This gives a measure of how accurately the assumed transition matrix, F, describes the time evolution of the system. Typical model errors vary from ignoring oceanic induced motion, to errors resulting from the quantization of the array into a finite number of segments. If these errors are modeled well then the diagonal terms of the error covariance matrix (see later) obtained as the solution to the Riccati equation, will give a good approximation to the mean square error of the estimated displacements of each of the array segments in practice. If the model errors are not well represented then this will not necessarily be the case. However, even in this latter case, the results can still be of use, in that they may determine general features, without giving accurate predictions, of the likely performance of the Kalman filter.

The simplying assumption is made that model errors are independent from segment to segment and from one time instant to another, i.e., the $\{\underline{w}(k)\}$ are uncorrelated and hence $Q = E\{\underline{w}(k)\underline{w}(j)^T\} = \sigma_p^2 I\delta_{kj}$, where δ_{kj} is the unit delta function. Such an assumption is also known to introduce robustness to a variety of modeling errors in the Kalman filter [12]. As discussed in [23], for the water pulley model we have $\sigma_p^2 = \sigma_p'^2/M$, where $\sigma_p'^2$ is the mean square model error over the whole array. Models errors due to the use of Euler differences are discussed in detail in [23] for the water pulley model.

D. Measurement Equation

To complete the state space representation of the system, the output of the jth sensor, denoted as $z_j(k)$ must be related to the states of the system, i.e., $\underline{\eta}(k)$. Note the jth sensor can be either a compass or a depth sensor. In the linear systems approach this relationship takes the form

$$\underline{z}(k) = H^T\underline{\eta}(k) + \underline{v}(k)$$

where H is the measurements matrix and $\underline{v}(k)$ represents sensor noise.

a) Displacement Sensors (e.g., Depth Sensors): Consider a set of K sensors that measure the transverse displacement and are located at positions $p_1h_\xi, p_2h_\xi, \cdots, p_Kh_\xi$ along the array with $p_1 < p_2 < p_K$ where the p_js are integers. In this case the $M \times K$ measurement matrix, H, takes the form

$$H_{mj} = \delta_{mp_j} \qquad m = 1, 2, \cdots, M. \quad \text{and} \quad j = 1, 2, \cdots, K.$$

Note that H can be written as

$$H^T = [I_K|0]P_{1p_1}P_{2p_2}\cdots P_{kp_k}$$

where P_{jp_j} is a permutation matrix which interchanges the jth and the p_jth rows of a vector and I_K is the $K \times K$ identity matrix.

b) Slope Sensors (e.g., Compasses): Here we consider K sensors located as above, but instead, the noise free output of the sensor is the slope of the array at the points $p_1h_\xi, p_2h_\xi, \cdots, p_Kh_\xi$. The noise free output of the p_jth sensor, $s_j(k)$, can be related to the state vector by the following approximation

$$s_j(k) = \left.\frac{\partial\eta}{\partial\xi}\right|_{\xi=p_jh_\xi,\,\tau=kh_\tau} \cong \frac{1}{h_\xi}(\eta_{p_j}(k) - \eta_{p_j-1}(k)).$$

Thus the measurement matrix, H, takes the form

$$H_{mj} = \frac{1}{h_\xi}(\delta_{mp_j} - \delta_{mp_j-1}).$$

(Note for a compass at the leading end of the array, i.e., the tow point, a forward difference approximation for the slope would probably suffice, or, alternatively the compass output could be considered as a driving term. Again, H can be written

$$H^T = \frac{1}{h_\xi}\{[I_K|0] - [L_K|0]\}P_{1p_1}P_{2p_2}, \cdots, P_{kp_k}.$$

where L_K is the $K \times K$ lowering operator with 1's along the first lower minor diagonal. A combination of position and slope sensors can easily be handled by combining the forms of the above measurements matrices.

The final term in the measurement equation, i.e., $\underline{v}(k)$, represents additive noise associated with the measuring device, henceforth we will refer to this as sensor noise. The form of $\underline{v}(k)$ is very dependent on the particular instrument used, e.g., for compasses, it may represent quantization noise associated with a finite word-length used in the transmission of the data or it may represent oscillations due to the rotation of the compass relative to the earth's magnetic field. Such specific considerations, since they depend on the detailed construction of the instrument, are beyond the scope of this paper and we only consider simple expressions for the measuring noise. In particular the noise is modeled as uniform and white, uncorrelated from sensor to sensor and uncorrelated with the noise free component of the output of the sensor, i.e., the $\{\underline{v}(k)\}$ are uncorrelated and hence $E\{\underline{v}(k)\underline{v}(j)^T\} = \sigma_m^2 I\delta_{kj}$.

E. Summary of the Linear Systems and Kalman Filter Approach

The approach outlined in the above sections is summarized in Fig. 4. The first step has been to discretize the array into a finite number of segments and to form a state space representation in which the states, $\eta_j(k)$, are the transverse displacement of each segment, $j = 1, 2, \cdots, M$ at discrete times $k\tau_0$. The evolution of the states in time is determined by the transition matrix, F, and the driving term $\underline{u}(k)$. The form of the transition matrix F is derived from the Paidoussis equation and, for many problems of practical interest, takes a simple form, reflecting the propagation of transverse motion down the array.

The measurement equation relates the states to the measured outputs of compasses or depth sensors located along the array through a matrix H. Again, this matrix usually has a simple form.

Given the state space representation a Kalman filter may be derived which recursively predicts the state of the system one time interval ahead, i.e., at time $k + 1$. This estimator,

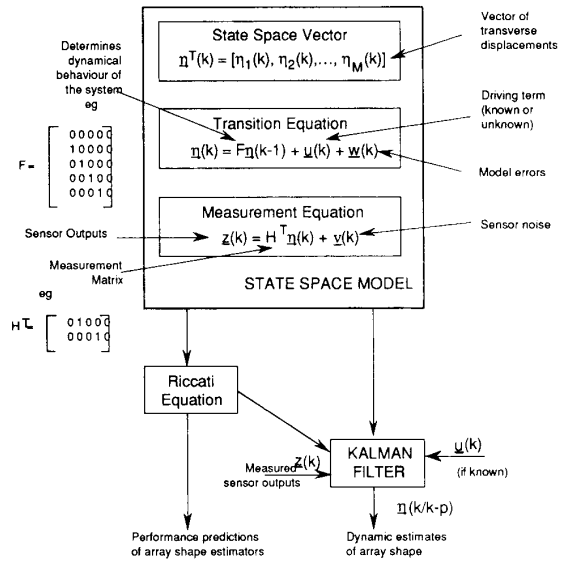

Fig. 4. Summary of Kalman filter approach.

denotes as $\underline{\eta}(k+1/k)$, is optimal in the sense that it has the least mean square prediction error conditional on all previous measurements up to time k, i.e., the set $Z(k) = \{\underline{z}(k), \underline{z}(k-1), \cdots, \underline{z}(0)\}$. See [12] and [23] for more details of the form of the Kalman filter. Prediction might be used to estimate the array shape one time interval ahead in order to allow the correct beamforming delays (or phase weights for frequency domain beamforming) to be precalculated.

Important extensions are filtering and fixed lag smoothing. In filtering, the state at time k given the set $Z(k)$, is estimated; this estimator is denoted by denoted as $\eta(k/k)$. In the array shape problem, filtering is probably the most likely technique to be used, since the array shape would not change much in the time taken to recompute the delay taps for a beamformer.

In cases where a time delay, of N samples, between the observations and the requirement for an estimate of the state is permissible, fixed lag smoothing can be used. In this case, an estimate of $\underline{\eta}(k-N)$: the state at time $k-N$ given all observations up to time k, is required. Fixed lag smoothing reduces the variance of the estimates of the array displacements. For this approach considerable expansion (depending on N) of the Kalman filter is required; the details are somewhat mathematical and are omitted here, see [12] and [23]. In the array shape problem fixed lag smoothing could be used in post trials analysis of digital data by using the recorded sensor outputs at some time to estimate the array shape at time $k-N$ and to beamform the stored acoustic data collected at time $k-N$. For at sea applications the time delays and data storage requirements would generally be unacceptable. The solution of the appropriate Riccati equation is used, in conjunction with a further linear matrix equation, to determine the reduction in variance that results form fixed lag smoothing. These errors can then be used to determine the trade off between improvements due to smoothing and losses due to the change in array shape over the smoothing period.

Defining Σ_p as the error covariance matrix of the $\underline{\eta}(k+1/k)$, i.e.,

$$\Sigma_p = E\{(\underline{\eta}(k) - \underline{\eta}(k+1/k))(\underline{\eta}(k) - \underline{\eta}(k+1/k))^T / Z(k)\}$$

it can be shown [12] that Σ_p is the solution of a time invariant derivative of the Riccati equation. It is shown in [12], and can be seen from the above, that although Σ_p is defined as conditional upon the set $Z(k)$, it is, in fact, an unconditional estimate of the error covariance matrix. It is this fact that makes it so useful in practice, as, for a given set of model parameters, it can be precomputed and thus can be used as a design tool for investigating the effect of changes in the model parameters on the variance of the errors in the state estimates. Furthermore the error covariance matrix for either filtered or fixed lag smoother estimators can be derived from Σ_p. In the time invariant case it is possible to determine the mean square error when all the time samples of the process, including those in the infinite future, are available. This error covariance provides a limit to the improvements that result from smoothing and it is simply determined from the steady state predictor error covariance, Σ_p, and the solution of the discrete time Lyapunov equation, see [12] and [23]. As will be seen later, how much future data is required for the array shape estimation problem can readily be related to the physics of the propagation of effects down the array.

IV. Discretization of the Array Slope

In the above application of the linear system representation, the states were the transverse displacements of the discretized array segments. For some beamforming and passive ranging applications, the slope of each segment may be of more interest. This may be particularly true for an array designed to carry out ranging by triangulation on bearing estimates for two or more well separated sub-arrays. Here, we show how the above model can be used to derive a state space representation in which the states of the system are the slopes of individual segments. First, consider the array discretized into M segments, as illustrated in Fig. 3, where we desire to estimate the slope for each segment. Defining the slope $\eta_\xi(\tau, \xi)$, by $\eta_\xi(\tau, \xi) = (\partial\eta(\tau, \xi)/\partial\xi)$ the state vector is given by

$$(\eta_\xi(k))_j = \left.\frac{\partial\eta(\tau, \xi)}{\partial\xi}\right|_{\xi = jh_\xi,\, t = kh_\tau}$$

for $j = 1, 2, \cdots, M$. The time variation of $\eta_\xi(\tau, \xi)$ can readily be obtained by differentiating (5), giving

$$(\tilde{\rho} - 1)(\xi - 1)\frac{\partial^2\eta_\xi}{\partial\xi^2} + (2\tilde{\rho} - 1)\frac{\partial\eta_\xi}{\partial\xi} + \frac{\partial\eta_\xi}{\partial\tau} = 0.$$

Following the method of Section IV the above equation can be discretized to give a state space representation. The details are omitted here but are given in [23].

Again for TPI motion whose wavelength is long compared with the array length, it can be shown that $\eta_\xi(\tau, \xi)$ satisfies

$$\tilde{\rho}\frac{\partial\eta_\xi}{\partial\xi} + \frac{\partial\eta_\xi}{\partial\tau} = 0$$

which again results in the simple expression $F = (1-\rho)I+\rho L$, for the transition matrix. Again constraints on h_τ and h_ξ can be imposed and damping can be introduced to give a transition matrix of the form αL.

V. An Example and Discussion

Consider the problem of an array of length 100 m being towed through the water at a constant speed of either 8 or 16 knots (i.e., approximately 4 or 8 m/s). The array is kept at a nominal depth of, say 30 ms, by a leveling device mounted at the head of the array. Vibration isolation modules (VIMS) in the section of cable connecting the head of the array to the stern of the towing vessel only partially dampen vertical motion of the vessel due to a surface swell. This surface motion induces vertical motion at the head of the array and generates TPI motion which then propagates down the array. (Motion in the horizontal plane due to yaw is not considered here.) The array is instrumentated with K calibrated depth sensors that enable the vertical displacements of the array section to be measured. A typical swell period of 12 s results in a nondimensional frequency $\overline{f}(= (1/T)(L/U))$ of 1 or 0.5 at 8 or 16 knots, respectively. Recalling from Section II that $\overline{f}$ is also the ratio of the wavelength of the disturbance to the array length, suggests that at speeds of 8 knots and above Kennedy's water pulley model may be used to describe the array motion, i.e., the p.d.e. governing the array motion is given by

$$\tilde{p}\frac{\partial \eta}{\partial \xi} + \frac{\partial \eta}{\partial \tau} = 0.$$

As discussed in Section III, the water pulley model results in a transition matrix of the form $(1-\rho)I + \rho L$ which for $\rho = 1$ results in a particularly simple form. (Also, as discussed in [23], the choice $\rho = 1$ minimizes the discretization errors for a sinusoidal driving term.) This choice implies that the spatial and temporal discretization intervals are related; i.e.,

$$h_\xi = h_\tau\left(\frac{\pi c_t + c_n}{c_n}\right).$$

From [13], typically c_t is small compared with c_n, implying $h_\xi = h_\tau$. The physical interpretation of $\rho = 1$ should again be reemphasized: in dimensional units h_t is the time that it takes a disturbance to propagate a distance of h_x assuming a propagation speed of U m/s down the array. Some examples of various discretizations, expressed in dimensional units, which results in $\rho = 1$ are given in Table I below. (Note that h_t is the rate at which the depth sensor outputs are sampled and is often determined by the array instrumentation.) The choice of the number of segments and, hence h_x, is a balance between the dimension of the state space representation and the accuracy with which the array shape is required to be estimated. For example, if the array was instrumented with 20 hydrophones spaced 5 m apart it may well be that segmenting the array into 20 segments suffices for estimating the array shape to the required accuracy. (The use of the Riccati equation to determine the number of segments and resulting errors is discussed in [23]).

To summarize, the state space water pulley model for $\rho = 1$, and incorporating a damping coefficient as discussed in Section III, takes the form

$$\underline{\eta}(k+1) = \alpha L\underline{\eta}(k) + \underline{u}(k) + \underline{w}(k)$$

where $\underline{w}(k)$ is the vector of discretization and model errors and, for TPI motion, $\underline{u}(k)$, the driving term, is of the form

$$\underline{u}(k) = [\eta_0(k), 0, \cdots, 0]^T.$$

We consider two cases below, the first where the driving force, $\underline{u}(k)$, i.e., the displacement of the tow point, is known and the second where it is not. In this particular example the distinction between the two cases could depend on whether the leveling device is actively controlled or not.

TABLE I
Spatial and Temporal Discretization Parameters (100 m Array)

Number of Segments	Speed (Knots)	Speed (m/s)	h_x (m)	h_t (s)
5	8	4	20	5
5	16	8	20	2.5
10	8	4	10	2.5
10	16	8	10	1.25
100	8	4	1	0.25
100	16	8	1	0.125

A. Known Tow Point Disturbance

In this case, the simple form of the state transition matrix, i.e., $F = \alpha L$, allows an analytic solution for the time invariant Riccati equation to be obtained. From [23] the Riccati equation can be shown to reduce to

$$\Sigma_p = \alpha^2 L[\Sigma_p^{-1} + \sigma_m^{-2}HH^T]^{-1}L^T + \sigma_p^2 I \qquad (10)$$

where H^T has the form where H^T has the form

$$H^T = \begin{bmatrix} 0 & 1 & \cdot & 0 & \cdot & 0 & \cdot & 0 \\ 0 & 0 & \cdot & 1 & \cdot & \cdot & \cdot & \cdot \\ \cdot & \cdot & \cdot & \cdot & \cdot & \cdot & \cdot & \cdot \\ 0 & 0 & \cdot & 0 & \cdot & 1 & \cdot & 0 \end{bmatrix}$$
$$\begin{matrix} \uparrow & \uparrow & \uparrow \\ p_1 & p_2 & p_K \end{matrix}$$

and p_1, p_2, and p_k are the positions (in integer multiples of h_ξ) of the K depth sensors along the array. The terms σ_p^2 and σ_m^2 are the variance of the model and measurement noise discussed in Sections III.C and III.D, respectively.

General Results: Since HH^T is diagonal, then Σ_p a diagonal matrix is the solution of (10), and it can be verified that $\Sigma_p = \text{diag}\{d_1, d_2, \cdots, d_M\}$ has entries obtained recursively by

$$d_1 = \sigma_p^2$$
$$d_j = \frac{\alpha^2\sigma_m^2 d_{j-1}}{\sigma_m^2 + \delta_{j-1,\{p_k\}}d_{j-1}} + \sigma_p^2$$

or equivalently

$$d_j = \sigma_p^2 + \alpha^2 d_{j-1} - \sigma^2\frac{d_{j-1}^2}{d_{j-1}+\sigma_m^2}\delta_{j-1,\{p_k\}} \qquad (11)$$

where $\delta_{j,\{p_k\}} = 1$ if $j \in \{p_1, p_2, \cdots, p_K\}$ and is zero otherwise.

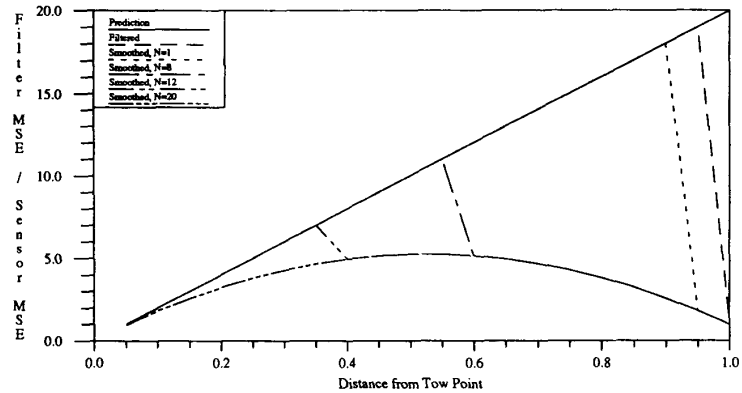

Fig. 5. Depth sensor at trailing end of array.

This latter expression allows terms to be readily identifiable, i.e.,

σ_p^2 is the contribution due to model errors,
$\alpha^2 d_{j-1}$ is the "propagation downstream" of the mean square error

and

$\frac{\alpha^2 d_{j-1}^2}{d_{j-1}+\sigma_m^2}\delta_{j-1,\{p_k\}}$ is the reduction in the mean square error (mse) of a particular segment due to a sensor in the previous upstream segment.

The expressions for the mse of the filtered estimates can readily be obtained from the mse of the one step predictor estimates by using the following equation [12];

$$\Sigma_f^{-1} = \Sigma_p^{-1} + HR^{-1}H^T$$

where Σ_f, the error convariance matrix of the filtered estimates, $\underline{\eta}(k/k)$, is defined in an analogous manner to Σ_p. The above equation implies that Σ_f is a diagonal matrix with diagonal elements, $\tilde{d}_j$, given by

$$\tilde{d}_j = \frac{\sigma_m^2}{\sigma_m^2 + \delta_{j,\{p_k\}} d_j} d_j. \tag{12}$$

The above expressions have some simple physical interpretations:

1) In the case of zero measurement noise, i.e., $\sigma_m = 0$, then $\tilde{d}_{p_j} = 0$, i.e., at the position of a perfect sensor there is zero mse.
2) From (12) the variance of the filtered estimates and of the predicted estimates differ only at points (segments) where a sensor is located. Thus the mean square error of the estimated displacement of a segment *not* containing a sensor is the same, irrespective of whether all information up to time k or time $k-1$ is used. This is a result of the assumption that for this model the time discretization is such that effects propagate from one spatial segment to another in the time discretization interval and so at time k the sensors outputs contain no more information regarding the position of other segments (not containing a sensor) than there was at time $k-1$.
3) As $\sigma_m \to \infty$, $\tilde{d}_{p_j}$ approaches d_{p_i}, the predicted value, i.e., a very noisy sensor does not reduce the variance of the filtered mse.
4) Note that a sensor at the end of the array although making the system observable, as discussed in the appendix, does not affect the d_j's and only reduces $\tilde{d}_j$ at the end of the array. It will however progressively reduce errors of the smoothed estimates as the lag of the smoother is increased. This will obviously reach a limit when the lag equals the time taken for an effect to transverse the length of the array.

Finally, by evaluating the Kalman gain matrix, for the damped water pulley model the predicted estimates of the state vector can be recursively written as

$$\eta_0(k/k-1) = (\underline{u}(k))_0$$

$$\eta_j(k+1/k) = \alpha\eta_{j-1}(k/k-1) + \frac{\sigma\delta_{j-1,\{p_k\}} d_{j-1}}{(d_{j-1}+\sigma_m^2)} \cdot \{z_q(k) - \eta_{j-1}(k/k-1)\}$$

where q is the ordered index of the depth sensor in the $j-1$th segment.

2) Specific Examples: In Figs. 5 and 6 the mean square errors are plotted as a function of segment number for a single sensor located at the midpoint and at the end of the array respectively. The array was discretized into 20 segments and $\alpha = 1$ and 0.95 respectively were used. By dividing through by σ_m^2 in (11) it can be seen that the normalised mean square errors depend on the ratio of the rms model error to the rms depth sensor error. Thus all results plotted are in units of σ_m^2, i.e., the variance of the depth sensor outputs. For these examples the variance of the model noise, σ_p^2, was assumed to be equal to that of the variance of the depth sensor noise, σ_m^2. Results for prediction, filtering, fixed lag smoothing, and infinite fixed lag smoothing are illustrated.

In Fig. 5, and subsequent figures, the results for prediction are the heavy line and form an upper bound to the errors. The lower bound is the result for the infinite fixed lag smoother.

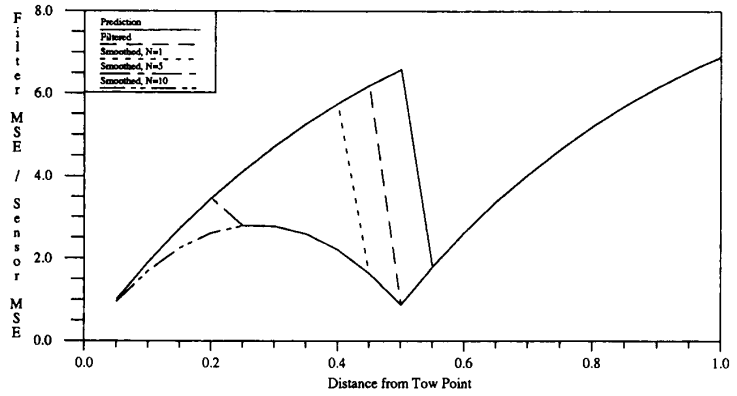

Fig. 6. Depth sensor at center of array.

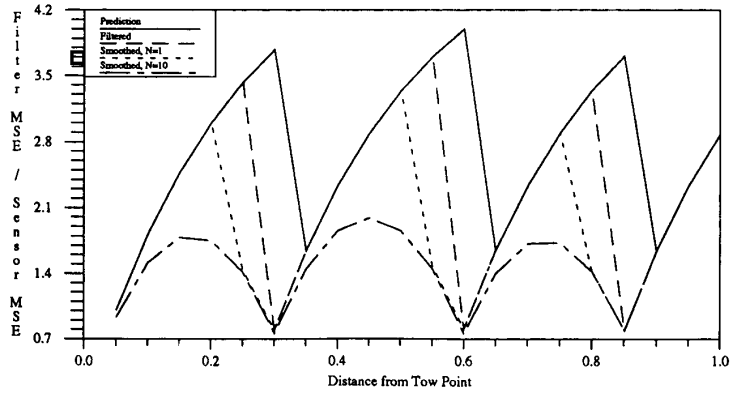

Fig. 7. Three depth sensors distributed along the array.

For the other estimators, the results initially coincide with the prediction results but then drop down to the lower bound with the transition point as indicated by the legend.

As Fig. 5 illustrates, a depth sensor located at the end of the array cannot reduce prediction errors, however for filtering the mean square error of the end segment is significantly reduced. For fixed lag smoothers of order 1, 8, 12, and 20 the reduction occurs for all segments 1, 8, 12, and 20 segments respectively upstream of the depth sensor. This can readily be interpreted in terms of the undamped propagation of disturbances down the array. The action of a fixed N-lag smoother can be interpreted as waiting for this disturbance to reach the depth sensor and then using that information to estimate the position of the upstream segment at the appropriate earlier instant in time. The distance upstream that can be estimated is determined by how many segments a disturbance can propagate in the time lag associated with the smoother. Note that as a corollary to this an infinite lag smoother will give identical results to an M-lag smoother where M is the maximum number of segments between any pair of adjacent sensors, in the above example this is 20.

The results for a depth sensor located at the midpoint of the array are shown in Fig. 6. As would be expected, the prediction errors downstream are reduced but those upstream are not, and are the same as those for Fig. 5 apart from the damping. Filtering decreases the mean square error at the midpoint and fixed lag smoothing progressively decreases the mean square error upstream of the depth sensor reaching the infinite lag smoother when the lag for the fixed lag smoother becomes equal to the time that it takes for a disturbance to propagate from the head of the array to the midpoint. Also neither filtering or fixed lag smoothing reduces the errors downstream of the depth sensor; all these results are identical and illustrate the liner accumulation of model errors.

In Fig. 7, the results for three depth sensors located at segment numbers 6, 12, and 17 are illustrated. A damping factor of 0.9 over one segment was assumed implying a damping of 0.12 over the whole array. Again the variance of the model error was assumed to be equal the variance of the depth sensor noise. The characteristic "opera house shells" are due to the damping factor and indicate the high initial growth of the model error. Similarly to Fig. 5 and 6, the results for all estimators are identical with the prediction results immediately downstream of a depth sensor but upstream drop down to the lower bound. The point at which this occurs is M lags upstream of any depth sensor. The results for prediction, filtering and fixed lag smoothing generalize the results presented earlier for a single sensor, i.e. prediction

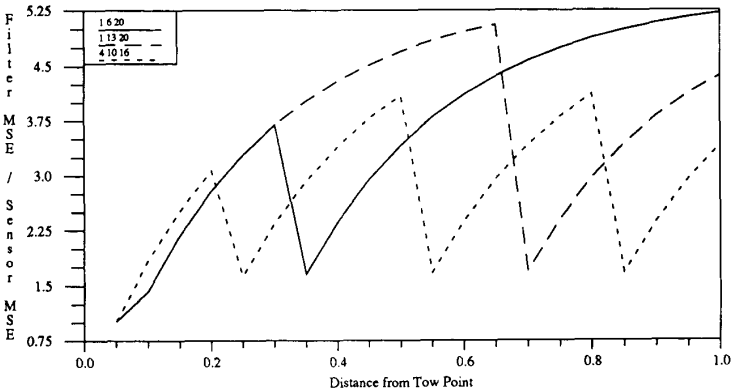

Fig. 8. Variation of sensor locations

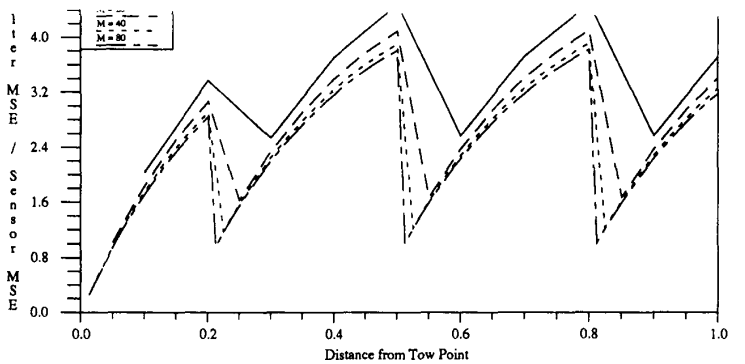

Fig. 9. Variation of number of segments.

reduces errors downstream, whilst smoothing reduces errors upstream with the smoothing results asymptoting when the smoothing lag equals the maximum separation of adjacent sensors.

The effect of varying the sensor positions is illustrated in Fig. 8. Here the parameters are the same as those used for Fig. 7 except that three different sets of sensor locations were considered; in terms of segment locations these were (1, 6, 20), (1, 13, 20), and (4, 10, 16). Only the results for prediction are shown and, as illustrated, the mean square error can be significantly reduced by the choice of sensors position.

Solutions to the Riccati equation also allow the effect of varying h_ξ, the spatial segment size, to be investigated. In Fig. 9 the mean square prediction errors when the array is discretized into 10, 20, 40, and 80 segments are illustrated. To ensure meaningful comparisons the damping constant was adjusted so that the same damping, 0.12, from the leading to trailing end of the array resulted. Also the mean square model error was adjusted by a factor of M as discussed in Section 3.C. The results indicate a reduction in errors as M is increased, but, for this example, above $M = 20$ the improvement is marginal. Further results presented in [23] illustrate how an increased damping coefficient or a noisier depth sensor results in a flattening of the "opera house shells."

B. Unknown Tow Point Disturbance

For unknown driving terms, i.e., unknown TPI motion, the Riccati equation becomes

$$\Sigma_p = \alpha^2 L[\Sigma_p^{-1} + \sigma_m^{-2} H H^T]^{-1} L^T + \sigma_p^2 I + U$$

where

$$U = \sigma_u^2 \begin{bmatrix} 1 & 0 & \cdot & \cdot & 0 \\ 0 & 0 & \cdot & \cdot & \cdot \\ \cdot & \cdot & \cdot & \cdot & \cdot \\ \cdot & \cdot & \cdot & \cdot & \cdot \\ 0 & \cdot & \cdot & \cdot & 0 \end{bmatrix}.$$

Again, from [23], Σ_p also is diagonal and the diagonal terms, i.e., the d_j's which are the variance of the estimated positions, are recursively given by (11) with d_1 being given by

$$d_1 = \sigma_p^2 + \sigma_u^2.$$

By inspection, it can readily be seen that the variance of the estimates of the array segment displacements are increased in proportion to the unknown driving term. This proportionality varies with the position of the segment along the array, the

damping and the position and the accuracy of the sensors. Note also

1) In the limit as $\sigma_u^2 \to 0$ the above equation reduces to (11), i.e., the known tow point disturbance results can be obtained by setting the mean power of the unknown driving term to zero.
2) For a noisy depth sensor located at the head of the array, i.e., $\sigma_m^2 \to \infty$ and for $\alpha = 1$ then

$$d_1 = \sigma_p^2 + \sigma_u^2, \quad d_2 = 2\sigma_p^2 + \sigma_u^2, \cdots \text{etc.}$$

Thus the error in the predicted estimates of the array segment displacements is the sum of the mean power of the unknown tow point disturbance and a linearly growing model error.
3) For filtering it can be shown that $d_1 \to 0$ and $d_j \to (j-1)\sigma_p^2$ as $\sigma_m \to 0$, i.e., with a highly accurate depth sensor, the displacements of all segments due to the tow point disturbance are estimated with a residual model error that grows linearly down the array.

C. Summary of Example Results

For all examples considered, the resulting errors of the prediction, filtered and smoothed versions of the Kalman filter can readily be interpreted in terms of the propagation of TPI motion down the array. The following conclusions, derived from the above examples and those given in [23], can be expected to hold quite generally.

For uniform sensors, the results depend on the ratio of model to sensor noise. Inherent in the Kalman filter approach is the prediction of the displacement of a given segment from the knowledge of the displacement of another segment upstream at an earlier time. Thus, in the application of the Kalman filter, there is an accumulation of model errors downstream in the estimates. The rate of increase of these errors depends on both the damping and the ratio of model to sensor noise. Unfortunately, for α not equal to unity, this rate is greatest just downstream of a sensor.

For either an accurate sensor located at the head of the array, or a known driving disturbance, the array shape errors are limited by model errors which grow geometrically down the array. Filtering or fixed lag smoothing of the outputs of sensors does not reduce errors downstream of the sensors below that of the predictor. However, upstream errors are reduced. The distance upstream that errors are reduced is determined by the number of lags used in the fixed lag smoother. Again this behavior can be interpreted in terms of the time taken for displacements to propagate from a point upstream to the sensor. Infinite fixed lag smoothing provides a limit to the improvements that result from smoothing; this limit being achieved when the lag equals the time taken for a disturbance to propagate the maximum distance between adjacent sensors.

VI. Summary

It has been shown that by discretizing the partial differential (Paidoussis) equation describing towed array dynamics, a Kalman filter may be designed that iteratively estimates the transverse distortion of the array due to motion induced at the tow point. When the wavelength of the induced motion is comparable or greater than the length of the array a particularly simple Kalman filter results and many properties of the Kalman filter reflect the physics of the propagation of disturbances down the array.

The solution of a Riccati type equation allows estimates of the mean square error of a segmented approximation to the array shape to be evaluated. These estimates have been quantified as functions of the model errors, the sensor errors, the position of the sensors along the array. These solutions are a useful design tool for deciding the locations and accuracies of compasses and depth sensors for instrumentating towed arrays.

VII. Appendix
Properties of the State Space and Kalman Filter Approach

Here stability conditions for both the linear systems approach and for the Kalman filter are derived. It is shown how observability of the system states is related to the physics of the propagation of TPI motion down the array.

A. Stability

First, consider stability from the linear systems point of view. In this context it is required that a bounded input produce a bounded output. The system is asymptotically stable if $|\lambda_m(F)| < 1$, where $\lambda_m(F)$ denotes the eigenvalue of maximum modulus of the time invariant transition matrix F of the signal model.

In the context of Kalman filtering (for either prediction, filtering or smoothing), the asymptotic stability requirement indicates that $\eta(k + p/k) \to \eta(k + p)$ as $k \to \infty$ in the absence of noise, i.e., the state estimates converge to the true estimates. From [12] the system is asymptotically stable if $[F, H]$ is detectable and $[F, Q^{1/2}]$ is stabilizable and it can be shown that a sufficient condition for both these technical requirements to hold is that $|\lambda_m(F)| < 1$.

In the case of the water pulley model we have, for $F = (1 - \rho)I + \rho L$,

$$\det(\lambda I - F) = (\lambda - 1 + \rho)^M.$$

Thus the eigenvalues are all equal to $1 - \rho$ and hence both system stability and Kalman filter stability are guaranteed if $|1 - \rho| < 1$, i.e. $-1 < \rho < 2$. Noting that

$$\rho = \tilde{\rho}\frac{h_\tau}{h_\xi}$$

it follows that the discretization must be such that the distance travelled by a disturbance during one temporal interval is less than twice the spatial step size. For the special case of $\rho = 1$, the spatial step size equals the distance travelled by a disturbance during one temporal step interval. As discussed in Section III.A, damping can readily be incorporated by multiplying L by the damping factor α. Also noting that the eigenvalues for a transition matrix of the form $F = \alpha L$ are all zero suffices to demonstrate asymptotic stability for the damped model.

B. Observability

In linear systems theory the concept of observability deals with the question of whether there can exist states of the system that cannot be determined from the measurements. In the problem addressed here, this means that given the outputs of the K measurement sensors, $\underline{z}(k)$, and the driving term $\underline{u}(k)$, whether it is possible to estimate all the components of $\underline{\eta}(k)$, i.e., the system states, at some earlier time, taken to be $k = 0$. Observability implies that knowledge of $\{\underline{u}(k)\}$ and $\{\underline{z}(k)\}$ for all k in some finite time interval suffices to determine $\underline{\eta}(0)$. Although in many practical applications of towed arrays the $\{\underline{u}(k)\}$, i.e., the driving term, is unlikely to be known, consideration of this concept does lead to some interesting physical insights which we now discuss.

Observability depends not only on the state transition matrix, but also on the positions of the sensors, i.e., the H matrix. From [12] the states of the system are unobservable if there exists a $\underline{w} \neq 0$ such that

$$H^T \underline{w} = 0$$

and

$$F\underline{w} = \lambda \underline{w} \text{ for some } \lambda.$$

To consider conditions on H such that the system is observable use the fact that F, H are observable if $F + \beta I$, H are also observable for some constant β. Taking $\beta = -1 + \rho$ for the water pulley model, it can readily be verified that all the eigenvalues of $F + \beta I$ are zero and all eigenvectors $\underline{w}$ are of the form $[0, 0, \cdots, 0, w_M]^T$. In this case, for $w_M \neq 0$,

$$H^T \underline{w} = 0$$

only if the last column of H^T is the zero vector. Hence, unless a measuring sensors is located at the trailing end of the array the system is unobservable, i.e., there can exist a $\underline{w}$ such that the system evolves as $\underline{w}, \lambda\underline{w}, \cdots, \lambda^M\underline{w}$, but since $H^T\underline{w} = 0$, this $\underline{w}$ can never be determined from the $z(k)$'s. For water pulley, whereby disturbances generated at the leading end of the array propagate down the array, this may seem strange, as it could be argued that a sensor at the leading edge of the array should suffice to predict all subsequent displacements of downstream sections of the array. However, the noise modeled in the system may be considered as "Lamb's demons" which can cause random, unknown perturbations to the shape predicted by an upstream sensor. Since the unknown displacements are assumed to only propagate aft, they would never be detected by a sensor forward of the generating point and hence would be unobservable. Thus a sensor at the rear is required, in principle, to observe these "Lamb's demons." In a practical situation the errors in the predicted array shape caused by not placing a sensor at the end of the array to observe the displacements caused by "Lamb's demons" may be tolerable and not warrant the expense and complication of placing an additional sensor at the end of the array.

As discussed above, observability comes from the concept that, given certain future outputs, the current state of the system can, in principle, be determined. In the array context this means that, given observations downstream (e.g., by positioning a sensor state the trailing end of the array), we can determine what the array position was upstream at some earlier instant. This concept is most useful for smoothing applications where a fixed time delay is allowable before the array shape estimates are required. In practical situations this point need to be carefully addressed. For example, in the off-line, post trial analysis of experimental data, in which much of the future is, in principle available, smoothing can be effectively used. The time constants of the smoothing are related to the times taken for effects to travel down the array. However, in real time system, where the array shape estimators are used in a dynamically programmable beamformer, or to adjust bearing or range estimates, the delays required for smoothing may be operationally too long. Furthermore, such an approach may not be practically feasible, in the sense that it is impossible to store all the data needed for beamforming with the smoothed estimate of the array shape.

ACKNOWLEDGMENT

Dr. J. Riley of the Australian Defence Science and Technology Organization is thanked for providing Figure 2: the solution to the Paidoussis equation and for many other useful discussions. M. Balin of the Cooperative Research Centre for Robust and Adaptive systems is thanked for computing the solutions to the Riccati equation.

REFERENCES

[1] S. M. Kay and H. C. Woodsum, "Sonar technology," in *Trends and Perspectives in Signal Processing*, pp. 1–7, Sept. 1993.
[2] W. H. Dragoset and K. L. Larner, "Data enhancement from a 500 channel streamer," *IEEE, J. Oceanic Eng.*, OE-9, pp. 40–47, Jan 1984.
[3] R. A. Monzingo and T. W. Miller, *Introduction to Adaptive Arrays*. New York: Wiley, 1980.
[4] N. L. Owsley, "Sonar array processing," *Array Processing Systems*. Englewood Cliffs, NJ: Prentice-Hall Inc., 1984, ch. 3.
[5] D. H. Johnson and S. DeGraaf, "Improving the resolution in bearing in passive sonar array by eignenvalue analysis," *IEEE Trans.*, vol. ASSP-30, pp. 638–647, 1982.
[6] M. J. Hinich, "Passive range estimation using subarray parallax," *J. Acust. Soc. Am.*, vol. 65, pp. 1229–1230, 1979.
[7] J. C. Hassab, "The effect of uncertainty in the heading or placement of a sub-array on passive ranging accuracy," *J. Acoust. Soc. Am.*, vol. 75, no. 2, pp. 479–485, 1984.
[8] N. L. Owsely, "Shape estimation for a flexible underwater cable," *1981 IEEE EASCON*, Nov. 16–19, Washington, DC.
[9] R. M. Kennedy, "Crosstrack dynamics of a long cable towed in the ocean," *Oceans*, pp. 966–970, 1981.
[10] M. P. Paidoussis, "Dynamics of flexible slender cylinder in axial flow; Part I theory," *J. of Fluid Mechanics*, vol. 26, pp. 717–736, 1966.
[11] M. P. Paidoussis, "Dynamics of flexible cylinders in axial flow; Part II experiment," *J. of Fluid Mechanics*, vol. 26, pp. 737–751, 1966.
[12] B. D. O. Anderson and J. B. Moore, *Optimal Filtering*. Englewood Cliffs, NJ: Prentice Hall, 1979.
[13] R. M. Kennedy and E. S. Strahan, "A linear theory of transverse cable dynamics at low frequencies," NUSC Tech. Rep. 6463, 1981. Naval Underwater Systems Center, New London, CT.
[14] J. Ketchman, "Vibration induced in towed linear underwater array cables," *IEEE, J. Oceanic Eng.*, vol. OE-6, pp. 77–87, July 1981.
[15] G. I. Taylor, "Analysis of the swimming of long and narrow animals," *Proc. Royal Soc. VA214*, pp. 158–183, 1952.
[16] H. P. Pao, "Dynamical stability of a towed thin flexible cylinder," *J. Hydronautics*, vol. 4, pp. 144, 1970.
[17] H. P. Pao and Q. Tran, "Response of a towed thin flexible cylinder in a viscous fluid," *J. Acoust. Soc., Am.*, vol. 53, no. 5, pp. 1441–14411, 1973.
[18] C. R. Ortloff and J. Ives, "On the dynamic motion of a thin flexible cylinder in a viscous stream," *J. Fluid Mechanics*, vol. 38, pp. 713–720, 1969.

[19] R. M. Kennedy and F. Galletta, "Cable dynamics experiment final report," NUSC Tech. Report 6467, 22 Oct. 1981, Naval Underwater Systems Center, New London, CT.
[20] D. Lee and R. M. Kennedy, "A numerical treatment of the dynamic motion of a zero bending rigidity cylinder in a viscous stream," NUSC Tech. Rep. 6343, 10 Feb. 1981, Naval Underwater Systems Center, New London, CT.
[21] A. P. Dowling, "The dynamics of towed flexible cylinders Part I. Neutrally buoyant elements," *J. of Fluid Mechanics*, vol. 187, pp. 507–532, 1988.
[22] A. P. Dowling, "The dynamics of towed flexible cylinders Part II. Negatively buoyant elements," *J. of Fluid Mechanics*, vol. 187, pp. 533–571, 1988.
[23] D. A. Gray, "Models for the application of Kalman filters to the estimation of the shape of a towed array," Australian Dept. of Defence Fellowship Rep., May 1986.
[24] R. J. Hansen and C. C. Ni, "Flow-induced transverse motions of a flexible cable aligned with the flow direction," *IEEE J. Oceanic Eng.*, vol. OE-4, pp. 152–156, Oct. 1979.
[25] R. R. Bitmead and B. D. O. Anderson, "Kalman filtering approaches for position estimation of towed arrays operating in damped water pulley mode," Interim Rep., April 1984, Department of Systems Engineering, Australian National University, Canberra, Australia.
[26] B. D. O. Anderson, "Commentary 'Lumped approximation of distributed systems and controllability questions," Rep. Aug. 1984, Department of Systems Engineering, Australian National University, Canberra, Australia.
[27] D. C. Miner, "Flexible solution seijic streamer control and positioning," *Sea Technology*, pp. 39–42, Aug. 1990.
[28] A. H. Kito van Hejningen, "Miniature heading sensors for new generation towed arrays," *Sea Technology*, pp. 47–50, Aug. 1990.
[29] J. L Riley, D. A. Gray, and D. A. Holdsworth, "Estimating the positions of an array of recievers using Kalman filtering techniques," *Proc. Int. Symp. on Signal Procesisng and Applications, ISSPA 90 (Bisbane, Australia)*, pp. 364–367, Aug. 1990.
[30] D. A. Gray, B. D. O. Anderson, and R. R. Bitmead, "Models for the application of Kalman filtering to the estimation of the shape of a towed array," *NATO Advanced Study Institute on Underwater Acoustic Data Processing* (Kingston, Ontario, Canada), July 18–29, 1988.

Douglas A. Gray (M'82) was born in the U.K. in 1946. He received the B.Sc. and Ph.D. degrees in mathematical physics from the University of Adelaide, South Australia, in 1969 and 1974, respectively.

From 1973 to 1993 he was with the Australian Defence Science and Technology Organization applying signal processing to sonar and electronic warfare. From 1977 to 1979 he was a visiting scientist at the Royal Aircraft Establishment, U.K. and in 1985 was a visiting fellow at the Australian National University, Australia. He is currently Professor of Sensor Signal Processing at the University of Adelaide, South Australia and Deputy Director of the Cooperative Research Centre for Sensor Signal and Information Processing. His research interests are in the application of signal processing to sonar and electronic warfare, particularly in adaptive processes, beamforming and signal sorting and classification techniques.

Brian D. O. Anderson (S'62–M'66–SM'74–F'75) was born in Sydney, Australia, and received his undergraduate education at the University of Sydney and Stanford University.

Following completion of his education, he worked in industry in Silicon Valley and served as an assistant professor in the department of electrical engineering at Stanford. He was foundation professor of electrical engineering at the University of Newcastle, Australia form 1967 till 1981 and is now Professor of Systems Engineering at the Australian National University. His interests are in control and signal processing.

Dr. Anderson is a Fellow of the Royal Society, the Australian Academy of Science, Australian Academy of Technological Sciences and Engineering, and the Institute of Electrical and Electronic Engineers, and an Honorary Fellow of the Institution of Engineers, Australia. He holds a doctorate (honoris causa) from the Université Catholique de Louvain, Belgium. He is serving a term as President of the International Federation of Automatic Control from 1990 to 1993.

Robert R. Bitmead (S'79–M'79–SM'86–F'91) was born in Sydney in 1954. He received the B.Sc. degree in applied mathematics from the University of Sydney and the M.E. and Ph.D. degrees from the University of Newcastle, Australia, in 1976, 1977, and 1979, respectively.

He has been on the faculty of the Australian National University in Canberra since 1983, where he currently holds the position of Senior Fellow of Systems Engineering and is the Director of the Cooperative Research Centre for Robust and Adaptive Systems. He has held faculty positions at the University of Newcastle and James Cook University of North Queensland, and visiting positions at Cornell University, USA, and the University of Louvain, Belgium.

Dr. Bitmead has been a Subject Editor for the *International Journal of Adaptive Control and Signal Processing*, an Associate Editor of *Automatica*, and an Associate Editor of *IEEE Transactions on Automatic Control*. He is currently the Chairman of the IFAC Technical Committee on Mathematics of Control. His research interests encompass adaptive systems in control, signal processing and telecommunications, stochastic processes and multivariable control.